Inhibition of RANKL-induced osteoclastogenesis through the suppression of the ERK signaling pathway by astragaloside IV and attenuation of titanium-particle-induced osteolysis

MINGJUN LI[1*], WENGANG WANG[2*], LI GENG[1], YANRU QIN[1], WENJIE DONG[1], XUDONG ZHANG[1], AN QIN[2] and MINGZHI ZHANG[1]

[1]Department of Oncology, The First Affiliated Hospital of Zhengzhou University, Zhengzhou, Henan 450052; [2]Department of Orthopedics, Shanghai Key Laboratory of Orthopedic Implant, Shanghai Ninth People's Hospital, Shanghai Jiao Tong University School of Medicine, Shanghai 200011, P.R. China

Received January 18, 2015; Accepted August 13, 2015

DOI: 10.3892/ijmm.2015.2330

Abstract. Astragaloside IV (AS-IV) is a natural plant extract that enhances osteoblast activity, and therefore, has the potential to treat osteoclast-related diseases. Such diseases include osteoporosis, periodontal disease, rheumatoid arthritis and aseptic prosthesis loosening. However, data associating the effects of AS-IV on osteoclasts are limited. The aim of the present study was to assess the effect of AS-IV on osteoclasts *in vitro* and *in vivo*. The *in vitro* studies demonstrated that AS-IV exerts potent inhibitory effects on the ligand of the receptor activator of nuclear factor-κB-induced osteoclastogenesis and revealed the mechanism of action of AS-IV, which inhibited osteoclastogenesis by suppression of the extracellular signal-regulated kinase signaling pathway. The *in vivo* studies proved that AS-IV attenuated titanium particle-induced osteolysis in a mouse calvarial model. Collectively, the findings of the study suggest that AS-IV is a potential natural agent for the treatment of osteoclast-related diseases.

Correspondence to: Professor Mingzhi Zhang, Department of Oncology, The First Affiliated Hospital of Zhengzhou University, 1 East Jianshe Road, Zhengzhou, Henan 450052, P.R. China
E-mail: mingzhi_zhang1@163.com

Dr An Qin, Department of Orthopedics, Shanghai Key Laboratory of Orthopaedic Implant, Shanghai Ninth People's Hospital, Shanghai Jiao Tong University School of Medicine, 639 Zhizaoju Road, Shanghai 200011, P.R. China
E-mail: dr.qinan@gmail.com

*Contributed equally

Abbreviations: AS-IV, astragaloside IV; BMMs, bone marrow macrophages; ERK, extracellular signal-regulated kinase; GAPDH, glyceraldehyde-3-phosphate dehydrogenase; MAPK, mitogen-activated protein kinase; M-CSF, macrophage colony-stimulating factor; NFATc1, nuclear factor of activated T cells c1; RANK, receptor activator of the nuclear factor-κB; RANKL, receptor activator of the nuclear factor-κB ligand; TNF, tumor necrosis factor; TRAF6, tumor necrosis factor receptor-associated factor 6

Key words: astragaloside IV, osteoclast formation, osteoclastic bone resorption, osteoclast-related diseases, extracellular signal-regulated kinase signaling, nuclear factor of activated T cells c1

Introduction

In vivo, the skeleton is constantly being remodeled via a process involving the breakdown (resorption) and build-up (synthesis) of bone, determined by a delicate balance between osteoblast and osteoclast activities (1). As osteoclasts have key roles in the regulation of bone mass and quality, the majority of adult skeletal diseases are due to excess osteoclast activity, resulting in osteopenia (2,3). Such diseases include osteoporosis, periodontal disease, rheumatoid arthritis and aseptic prosthesis loosening (4,5). For individuals with osteoporosis, a condition characterized by low bone mass and skeletal fragility, low trauma bone fractures represent life-threatening events, particularly when they affect the vertebrae, proximal femur (hip), distal forearm or proximal humerus (6).

Osteoclasts are large, multinucleated cells that arise from the hematopoietic stem cell monocyte/macrophage lineage (7). Osteoclast activation was initiated by activation of the receptor activator of the nuclear factor-κB (RANK) and RANK ligand (RANKL) signaling pathways (8,9). RANK and RANKL belong to the tumor necrosis factor (TNF) receptor superfamily (10,11). The binding of RANKL to RANK recruits the adapter protein, TNF receptor-associated factor 6 (TRAF6), to the plasma membrane. RANK, RANKL and TRAF6 are essential for osteoclastogenesis, as mice lacking these molecules show profound bone resorption defects (12). The RANK/TRAF6 complex activates several pathways, including NF-κB signaling and the mitogen-activated protein kinase (MAPK) pathways involving extracellular signal-related kinase (ERK), which induce expression of nuclear factor of activated T cells c1 (NFATc1), considered one of the master transcription factors controlling osteoclastogenesis (13-15). Therefore, ERK and NFATc1, which are closely regulated by MAPK activity, are essential for the differentiation, survival and activation of osteoclasts (16-18).

Astragaloside IV (AS-IV) (Fig. 1) is a saponin purified from *Astragalus membranaceus* Bge., one of the most widely used Chinese herbs (19). AS-IV has been reported to have a wide range of treatment effects, with no toxicity (20). Pharmacological activities attributed to AS-IV include cardioprotective (21), anti-inflammatory (22), antioxidant (23), anti-asthmatic (24) and anticancer (25) effects. Some of these pharmacological activities resulted from AS-IV-mediated inhibition of ERK (26-28) and NF-κB (26,29-31) signaling pathways. Furthermore, AS-IV has been reported to affect osteogenesis (32), and have anti-arthritis activity (33). All these findings indicated that AS-IV may have a negative effect on osteoclastogenesis and may therefore have a significant potential for the treatment of osteoclast-related diseases, including osteoporosis. However, to the best of our knowledge, there is little published information regarding this issue.

Therefore, the present study aimed to i) investigate the potential therapeutic benefits of AS-IV on osteoclast-related osteolytic bone diseases, ii) understand the underlying mechanisms mediating the effects of AS-IV on osteoclast formation and function, and iii) further elucidate the potential molecular mechanisms of AS-IV in osteoclasts.

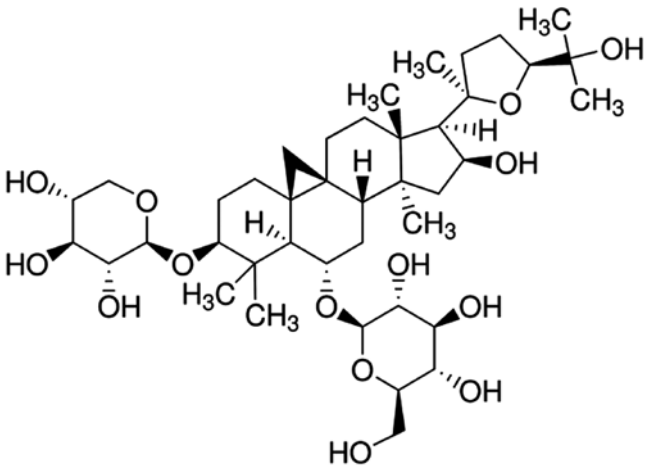

Figure 1. Chemical structure of astragaloside IV, with a molecular formula of $C_{41}H_{68}O_{14}$ and a molecular weight of 784.97 g/mol.

Materials and methods

Media, reagents and cells. Fetal bovine serum and α-modification of Eagle's medium (α-MEM) were obtained from Gibco-BRL (Sydney, Australia). The cell counting kit-8 (CCK-8) was purchased from Dojindo (Kumamoto, Japan). Soluble human recombinant macrophage-colony stimulating factor (M-CSF) and bacteria-derived recombinant mouse RANKL were supplied by R&D Systems (Minneapolis, MN, USA). AS-IV (purity >98%) was purchased from Sigma-Aldrich (St. Louis, MO, USA) and dissolved in dimethyl sulfoxide prior to dilution to the appropriate concentrations in culture medium (34). Western blot-specific antibodies were obtained from Cell Signaling Technology (Cambridge, MA, USA). RAW264.7 cells were purchased from the American Type Culture Collection (Rockville, MD, USA).

Cytotoxicity assay. The cytotoxic effects of AS-IV were determined using a CCK-8 assay. Bone marrow macrophages (BMMs) of C57/BL6 mice were seeded in 96-well plates at a density of $8x10^3$ cells/well, and cultured for 24 h. Cells were subsequently treated with different concentrations of AS-IV for 24, 48, 72 and 96 h. CCK-8 buffer (10 μl) was added to each well, and the cells were incubated at 37˚C for an additional 2 h. The absorbance was subsequently measured at a wavelength of 450 nm (650 nm reference). The half-maximal inhibitory concentration (IC_{50}) value was calculated.

BMM isolation and osteoclast culture. For primary cell culture, BMMs were obtained from the femurs and tibias of 6-week-old C57/BL6 mice. Cells were cultured in a T75 flask for 24 h. Floating cells were removed, and the adherent cells were cultured for another 3 days. The BMMs were subsequently seeded in a 96-well plate at a density of $8x10^3$ cells/well in complete α-MEM supplemented with 30 ng/ml M-CSF, 50 ng/ml RANKL and different concentrations of AS-IV (0, 25, 50 or 100 μM). Culture media were replaced every 2 days until mature osteoclasts had formed. Osteoclasts were identified by positive staining for tartrate-resistant acid phosphatase (TRAP). TRAP-positive cells with >3 nuclei were counted under a microscope.

F-actin ring immunofluorescence. For F-actin ring immunofluorescent staining, osteoclasts were fixed with 4% paraformaldehyde for 15 min at room temperature and permeabilized for 5 min with 0.1% v/v Triton X-100. Cells were incubated with rhodamine-conjugated phalloidin (1:100; Invitrogen, Carlsbad, CA, USA) for 1 h at room temperature. Cells were subsequently incubated with Hoechst 3342 dye (1:5,000) for visualization of the nuclei, washed with phosphate-buffered saline (PBS), and mounted with ProLong Gold anti-fade mounting medium (both from Invitrogen). Fluorescence detection was performed on Nikon A1Si spectral detector confocal system equipped with 20X (dry) lenses (Nikon, Tokyo, Japan). Images were collected using NIS-C elements software and analyzed using ImageJ Software (National Institutes of Health, Bethesda, MD, USA).

Bone resorption pit assay. BMMs were seeded on bone slices in 96-well plates at a density of $8x10^3$ cells/well and stimulated (in triplicate) with M-CSF (30 ng/ml), RANKL (50 ng/ml) and AS-IV (0, 25, 50 or 100 μM). Bone slices were imaged using field-emission scanning electron microscopy (FESEM, Hitachi S-4800, CamScan; Hitachi, Tokyo, Japan) with a magnification of 10 kV.

RNA extraction and reverse transcription-quantitative polymerase chain reaction (RT-qPCR) assay. RT-qPCR was used to measure specific gene expression. BMMs were plated in 6-well plates at a density of $1x10^5$ cells/well and cultured in complete α-MEM supplemented with 30 ng/ml M-CSF and 50 ng/ml RANKL. For the concentration gradient assay, cells were incubated with AS-IV (0, 25 or 50 μM) for 5-7 days until mature osteoclasts formed. For the time gradient assay, cells were incubated with 50 μM AS-IV for 0, 1, 3 or 5 days. Total RNA was extracted using the Qiagen RNeasy Mini kit (Qiagen, Valencia, CA, USA) and cDNA was synthesized from 1 μg of total RNA using reverse transcriptase (Takara

Biotechnology, Otsu, Japan). qPCR was performed using the SYBR Premix Ex Tag kit (Takara Biotechnology) and an ABI 7500 Sequencing Detection system (Applied Biosystems, Foster City, CA, USA) with 40 cycles of denaturation at 95˚C for 5 sec and amplification at 60˚C for 24 sec. GAPDH was used as the reference gene, and all the reactions were run in triplicate. The mouse primer sequences for cathepsin K (CtsK), TRAP, dendritic cell-specific trans membrane protein (DC-STAMP), V-ATPase d2, c-fos, NFATc1 and GAPDH were as follows: CtsK forward, 5'-CTTCCAATACGTGCA GCAGA-3' and reverse, 5'-TCTTCAGGGCTTTCTCGTTC-3'; TRAP forward, 5'-CTGGAGTGCACGATGCCAGCGACA-3' and reverse, 5'-TCCGTGCTCGGCGATGGACCAGA-3'; DC-STAMP forward, 5'-AAAACCCTTGGGCTGTTCTT-3' and reverse, 5'-AATCATGGACGACTCCTTGG-3'; V-ATPase d2 forward, 5'-AAGCCTTTGTTTGACGCTGT-3' and reverse, 5'-TTCGATGCCTCTGTGAGATG-3'; c-fos forward, 5'-CCA GTCAAGAGCATCAGCAA-3' and reverse, 5'-AAGTAG TGCAGCCCGGAGTA-3'; NFATc1 forward, 5'-CCGTTG CTTCCAGAAAATAACA-3' and reverse, 5'-TGTGGGATG TGAACTCGGAA-3'; and GAPDH forward, 5'-ACCCAG AAGACTGTGGATGG-3' and reverse, 5'-CACATTGGG GGTAGGAACAC-3'.

NF-κB luciferase reporter assay. RAW264.7 cells were stably transfected with a p-NF-κB-TA-Luc luciferase reporter construct. Briefly, cells were plated in a 24-well plate at a density of $1x10^5$ cells/well. The cells were treated 24 h later with different AS-IV concentrations (0, 12.5, 25, 50, 100 or 200 μM) for 1 h, prior to incubation with 50 ng/ml RANKL for a further 8 h. Cells were subsequently lysed and luciferase activity was measured using the Promega Luciferase Assay system (Promega, Madison, WI, USA).

Western blotting. RAW264.7 cells were seeded in 6-well plates at a density of $5x10^5$ cells/well. After pretreatment with or without AS-IV (200 μM) for 4 h, the cells were stimulated with RANKL for 0, 5, 10, 20, 30 or 60 min. The cells were subsequently washed twice in PBS and lysed in radioimmunoprecipitation assay lysis buffer. The lysates were centrifuged at 12,000 x g for 15 min and supernatants were collected.

Protein concentrations were determined using the bicinchoninic acid assay. Protein from each lysate (20 μg) was resolved using 10% sodium dodecyl sulfate-polyacrylamide gel electrophoresis gels, and transferred to polyvinylidene difluoride membranes (Millipore, Bedford, MA, USA). Membranes were subsequently blocked with 5% skimmed milk in TBS-Tween-20 for 1 h, and incubated with primary antibodies overnight at 4˚C. The membranes were incubated with horseradish peroxidase-conjugated secondary antibodies (1:5,000) for 1 h. Antibody reactivity was detected using an Odyssey infrared imaging system (LI-COR Biosciences, Lincoln, NE, USA).

Titanium particle-induced calvarial osteolysis model. An *in vivo* wear particle-induced osteolysis model was generated as previously reported (35). All the animal care and experimental procedures complied with Directive 2010/63/EU revising Directive 86/609/EEC approved by Animal Care and Use Committee of Zhengzhou University (approved on Feb 19th 2014, the approval number is 001381) . Twenty healthy 8-week-old C57BL/J6 mice were randomly assigned to four groups: Sham PBS control (sham), Ti particles with PBS (vehicle), and Ti particles with low (10 mg/kg/day) and high (25 mg/kg/day) concentrations of AS-IV (low and high, respectively). AS-IV was used by intraperitoneal injection every other day for 14 days. At the end of the experiment, the mice were sacrificed, and the calvaria were excised and fixed in 4% paraformaldehyde for micro-computed tomography (micro-CT) analysis.

Micro-CT scanning. A high-resolution micro-CT scanner (Skyscan 1176; Skyscan; Aartselaar, Belgium) was used with the following settings: X-ray voltage, 50 kV; electric current, 500 mA; and rotation step, 0.7˚. Following reconstruction, a square region of interest (ROI) around the midline suture was chosen for further qualitative and quantitative analyses. The bone volume against tissue volume (BV/TV), number of porosities and percentage of total porosity were determined for each sample as described previously (36).

Statistical analysis. The data Are expressed as mean ± standard deviation. The results were analyzed using the analysis of variance and post hoc tests with the SPSS 13.0 software (SPSS Inc., Chicago, IL, USA). $P<0.05$ was considered to indicate a statistically significant difference between groups.

Results

AS-IV cytotoxicity. CCK-8 cell viability assays were performed to examine the potential AS-IV cytotoxicity. The results showed that AS-IV cytotoxicity was concentration- and time-dependent (Fig. 2). These assays indicated that the maximum concentration used in the subsequent studies (200 μM) showed no cytotoxic effects in BMMs, even after 96-h exposure. Based on these data, the AS-IV concentrations used in subsequent experiments were considered non-cytotoxic.

Effect of AS-IV on osteoclastogenesis. As osteoclasts have key roles in osteoclast-related diseases (2), the effect of AS-IV on osteoclastogenesis was investigated. BMMs were exposed to AS-IV (0, 25, 50 and 100 μM) during osteoclast formation. The control group formed numerous TRAP-positive multinucleated osteoclasts (Fig. 3A). Osteoclast formation was inhibited by AS-IV (Fig. 3A-C). Furthermore, comparison of the control and 100 μM AS-IV cells after 3, 5 and 7 days produced similar results (Fig. 3D-F).

F-actin ring formation. To further examine the effects of AS-IV on osteoclastogenesis, RANKL-induced osteoclast F-actin ring formation was studied, which is the most well-known characteristic of mature osteoclasts and a prerequisite for osteoclast bone resorption during osteoclastogenesis (37). As expected, confocal microscopy revealed F-actin ring formation and characteristic podosomal condensation in control osteoclasts. However, the size and number of F-actin rings significantly decreased in cells incubated with AS-IV (Fig. 4A), suggesting that AS-IV suppressed F-actin ring formation.

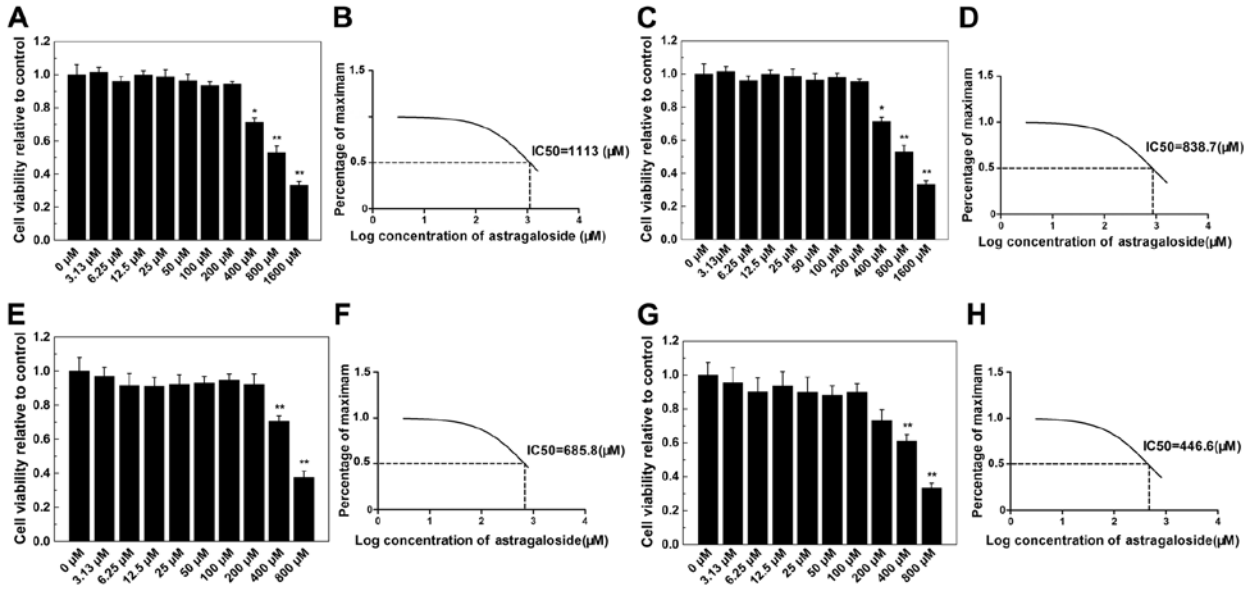

Figure 2. Cytotoxic assays of AS-IV treatment. (A) BMMs were cultured in complete α-modification of Eagle's medium medium containing the indicated concentrations of AS-IV for 24 h. The cell viability, relative to control, was measured by the CCK-8 assay. (B) The inhibition rate of BMMs was calculated using GraphPad Prism software, and the IC_{50} was 1,113 μM. (C) BMM cell viability relative to control was measured by the CCK-8 assay following 48 h incubations with the indicated concentrations of AS-IV. (D) The AS-IV IC_{50} at 48 h was 838.7 μM. (E) The cell viability relative to control was measured by the CCK-8 assay following 72 h incubations with the indicated concentrations of AS-IV. (F) The AS-IV IC_{50} at 72 h was 685.8 μM. (G) The cell viability relative to control was measured by the CCK-8 assay following 96 h incubations with the indicated concentrations of AS-IV. (H) The AS-IV IC_{50} at 96 h was 446.6 μM. *P<0.05 and **P<0.01, compared to 0 μM treatment (control). AS-IV, astragaloside IV; BMMs, bone marrow macrophages; CCK-8, cell counting kit-8; IC_{50}, half-maximal inhibitory concentration.

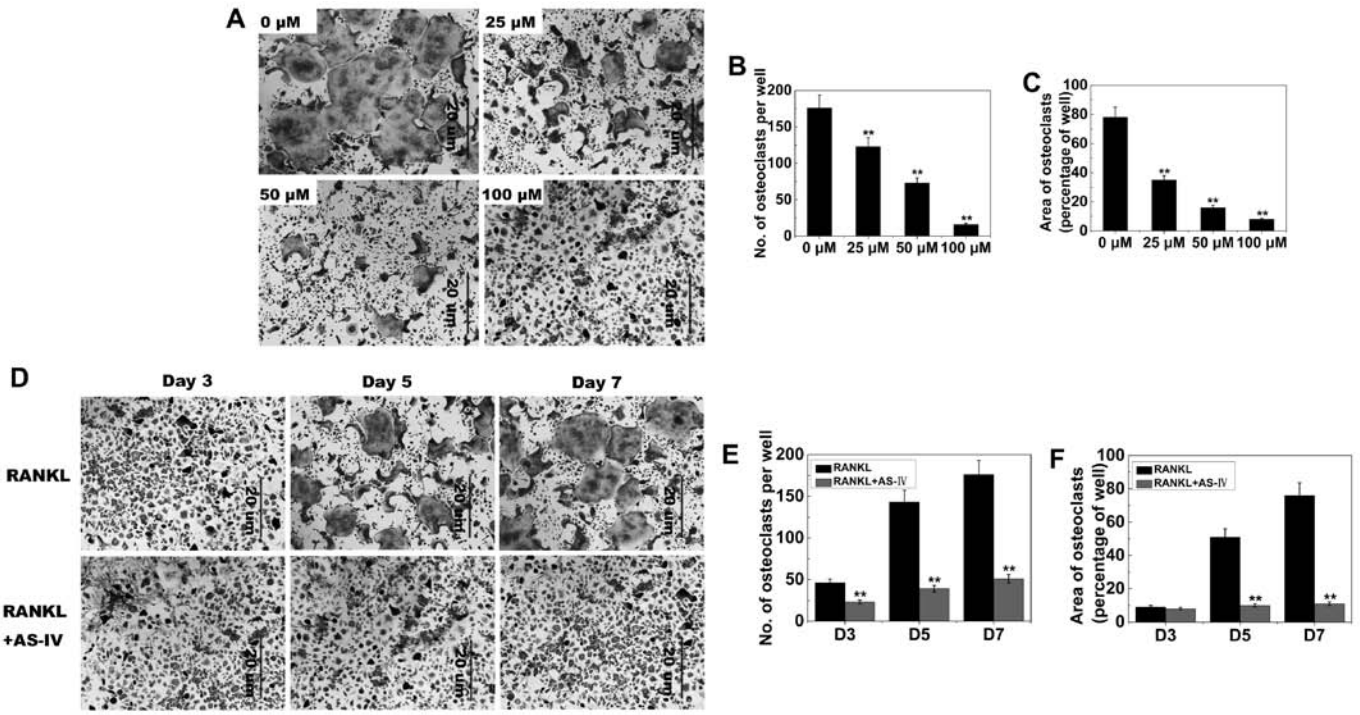

Figure 3. AS-IV inhibits RANKL-induced osteoclastogenesis. (A) BMMs were treated with different concentrations of AS-IV followed by 30 ng/ml M-CSF and 50 ng/ml RANKL for 5-7 days. Cells were subsequently fixed with 4% paraformaldehyde and stained for TRAP. (B) The number of TRAP-positive cells. (C) The area occupied by TRAP-positive cells. (D) BMMs were treated with or without 100 μM AS-IV, followed by 30 ng/ml M-CSF and 50 ng/ml RANKL. Cells were subsequently fixed and stained for TRAP on days 3, 5 and 7. (E) The number of TRAP-positive cells at the indicated time-points. (F) The area occupied by TRAP-positive cells at the indicated time-points. **P<0.01, compared to 0 μM treatment (control). AS-IV, astragaloside IV; RANKL, receptor activator of the nuclear factor-κB ligand; BMMs, bone marrow macrophages; M-CSF, macrophage colony-stimulating factor; TRAP, tartrate-resistant acid phosphatase.

Osteoclast bone resorption. As the formation of a well-polarized F-actin ring is an essential prerequisite for efficient bone resorption by osteoclasts, we inferred that osteoclast bone resorption would also be inhibited by AS-IV. Numerous bone resorption pits were observed on the surface of control bone slices (Fig. 5). In bone slices exposed to AS-IV, the resorption

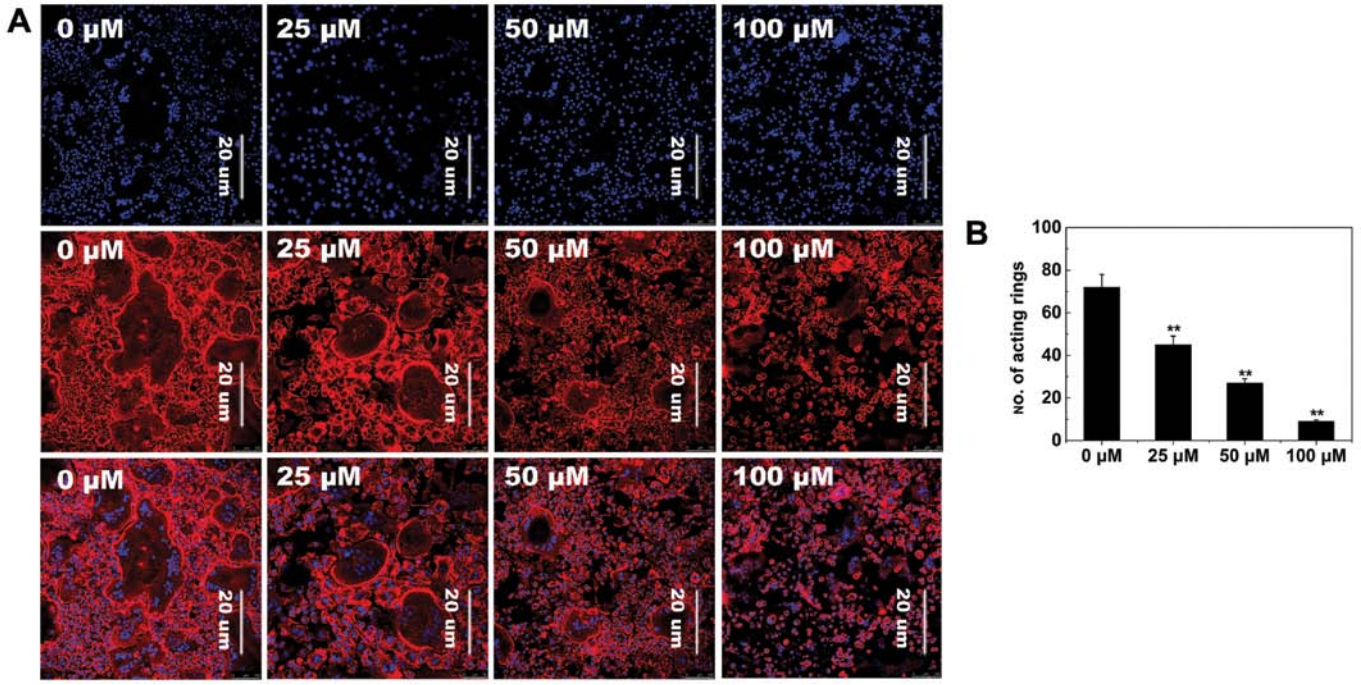

Figure 4. Astragaloside IV inhibits RANKL-induced F-actin ring formation. (A) Bone marrow macrophages were incubated with macrophage colony-stimulating factor (30 ng/ml) and RANKL (50 ng/ml), followed by treatment with or without AS-IV. Cells were fixed and stained for F-actin. (B) The number of osteoclasts with F-actin rings. *P<0.05 and **P<0.01, compared to 0 μM treatment (control). RANKL, receptor activator of the nuclear factor-κB ligand.

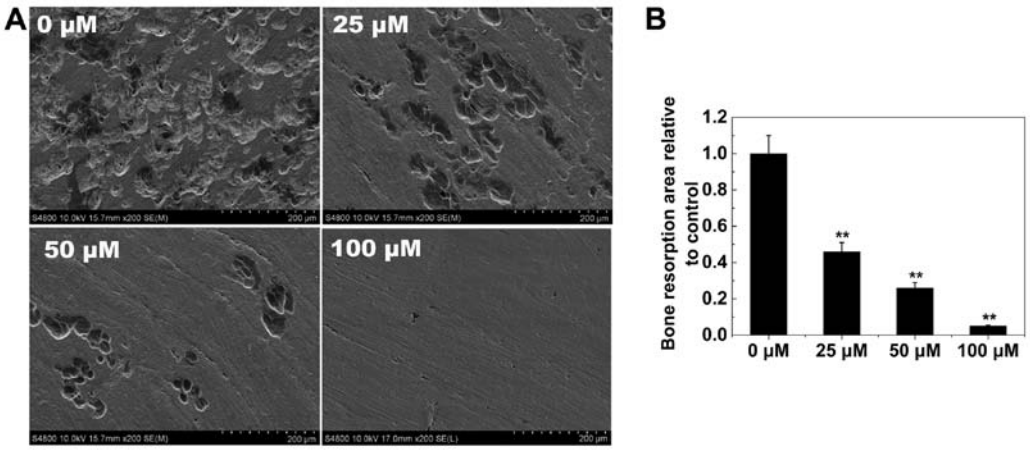

Figure 5. Astragaloside IV inhibits osteoclast bone resorption. Resorption pit areas were measured using ImageJ software. All the experiments were performed at least three times. (A) Representative scanning electron microscopy images of bone resorption pits. (B) The bone resorption area, relative to control. **P<0.01, compared to 0 μM treatment (control).

area was decreased. These findings demonstrated that AS-IV impaired osteoclast bone resorption *in vitro*.

RANKL-induced gene expression. The expression levels of several specific genes are upregulated during osteoclast differentiation. Thus, RT-qPCR was used to examine and quantify the RANKL-induced mRNA expression of osteoclast-related genes (including NFATc1, TRAP, V-ATPase d2, CtsK, DC-STAMP and c-fos). The results showed that the expression of these genes was inhibited by AS-IV in a dose- and time-dependent manner (Fig. 6).

RANKL-induced ERK and NFATc1 expression signaling. RANKL-induced activation of ERK is essential for osteoclast differentiation and function (38,39). The effects of AS-IV on RANKL-induced signaling pathways were therefore investigated. ERK phosphorylation increased within 5-30 min of stimulation with RANKL in the control group. However, ERK phosphorylation was significantly reduced by exposure to AS-IV (Fig. 7A). Quantitative analysis confirmed these results (Fig. 7C). These results suggested that AS-IV inhibited phosphorylation of ERK during osteoclast differentiation.

NFATc1 is an important master regulator of osteoclastogenesis and osteoclast function (40). Therefore, the effects of AS-IV on RANKL-induced NFATc1 expression were investigated. The data presented in Fig. 6A and B indicated that NFATc1 transcriptional activity increased when the cells were stimulated by RANKL. AS-IV inhibited this activity in

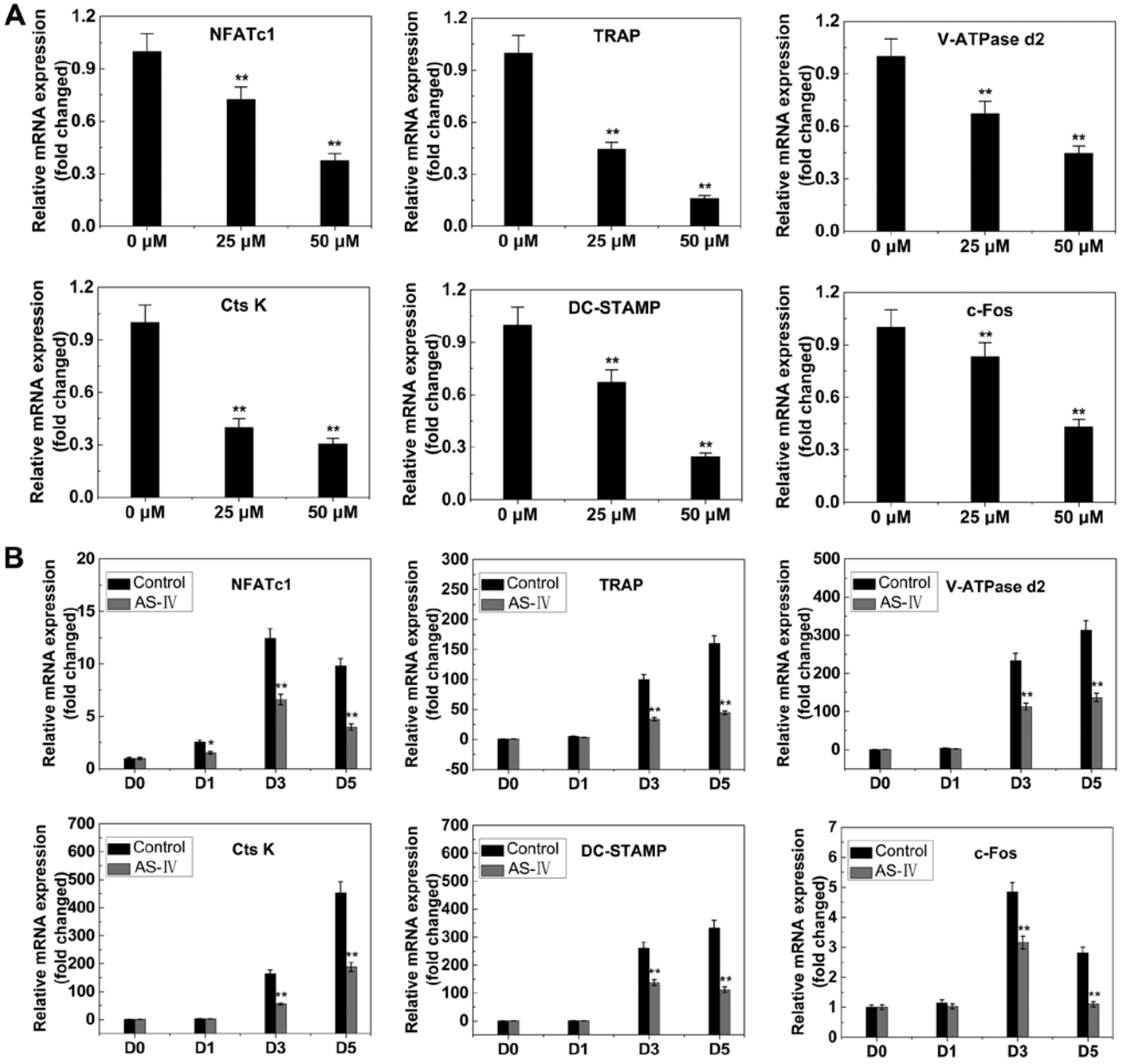

Figure 6. AS-IV suppresses RANKL-induced expression of osteoclast-specific genes. Bone marrow macrophages were cultured with macrophage colony-stimulating factor (30 ng/ml) and RANKL (50 ng/ml), with or without AS-IV. NFATc1, TRAP, V-ATPase d2, CtsK, DC-STAMP and c-fos expression levels were analyzed by reverse transcription-quantitative polymerase chain reaction and the results were normalized to the expression of glyceraldehyde-3-phosphate dehydrogenase. (A) Levels of the indicated mRNAs following exposure to AS-IV (0, 25 or 50 μM). (B) Levels of the indicated mRNAs following exposure to 50 μM AS-IV for 0, 1, 3 or 5 days. All the experiments were performed at least three times. *P<0.05 and **P<0.01, compared to 0 μM treatment (control). AS-IV, astragaloside IV; RANKL, receptor activator of the nuclear factor-κB ligand; TRAP, tartrate-resistant acid phosphatase; NFATc1, nuclear factor of activated T cells c1.

a dose- and time-dependent manner. To confirm this effect of AS-IV on NFATc1 expression, the NFATc1 protein level was examined using western blot analysis. NFATc1 protein levels increased when cells were exposed to RANKL, and AS-IV attenuated this increase (Fig. 7D and E), suggesting that AS-IV suppressed RANKL-induced NFATc1 expression.

RANKL-induced NF-κB signaling. RANKL-induced NF-κB activation is also a dominant mediator of osteoclast differentiation, resorption function and survival (41-43). Western blot analysis and luciferase assays were used to investigate the NF-κB signaling pathway. Similar levels of IκBα phosphorylation and degradation were observed in control and AS-IV groups (Fig. 7A). This observation was supported by luciferase reporter gene assays (Fig. 7B). These data indicated that AS-IV inhibited osteoclastogenesis without affecting the NF-κB signaling pathway.

Titanium particle-induced osteolysis. To explore the effects of AS-IV on pathological osteolysis, a Ti particle-induced mouse calvarial osteolysis model was used. The degree of particle-induced osteolysis was assessed using high-resolution micro-CT. Compared with the sham group (no Ti particles), the vehicle group (administration of Ti particles in PBS) showed significant calvarial osteolysis. When AS-IV (10 mg/kg, low; 25 mg/kg, high) was administered with the

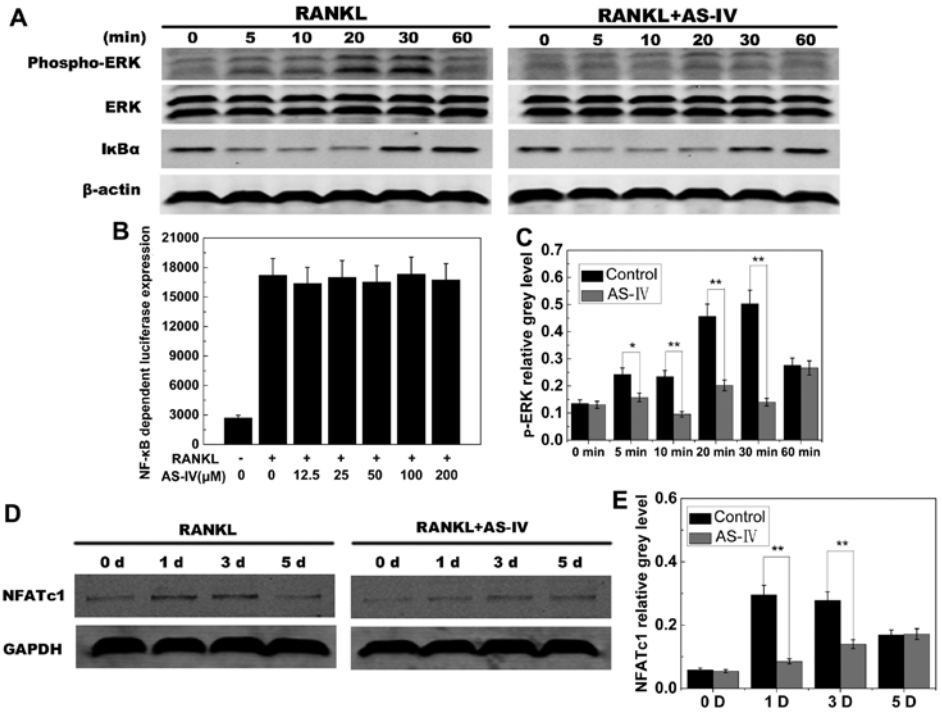

Figure 7. AS-IV-mediated suppression of RANKL-induced effects on ERK and NFATc1 signaling. (A) ERK phosphorylation increased within 5-30 min of stimulation with RANKL in the control group, and was significantly reduced by treatment with 200 μM AS-IV. The phosphorylation and degradation of IκBα was unaffected by exposure to 200 μM AS-IV. (B) Luciferase reporter assays showed that AS-IV did not affect RANKL-induced NF-κB signaling. (C) Quantitative analysis of ERK phosphorylation confirmed the data presented in (A). (D) Suppression of RANKL-induced NFATc1 signaling by AS-IV (200 μM). (E) Quantitative analysis of NFATc1 expression. *P<0.05; **P<0.01. AS-IV, astragaloside IV; RANKL, receptor activator of the nuclear factor-κB ligand; ERK, extracellular signal-regulated kinase; NFATc1, nuclear factor of activated T cells c1; IκBα, nuclear factor of κ light polypeptide gene enhancer in B-cells inhibitor α; NF-κB, nuclear factor-κB.

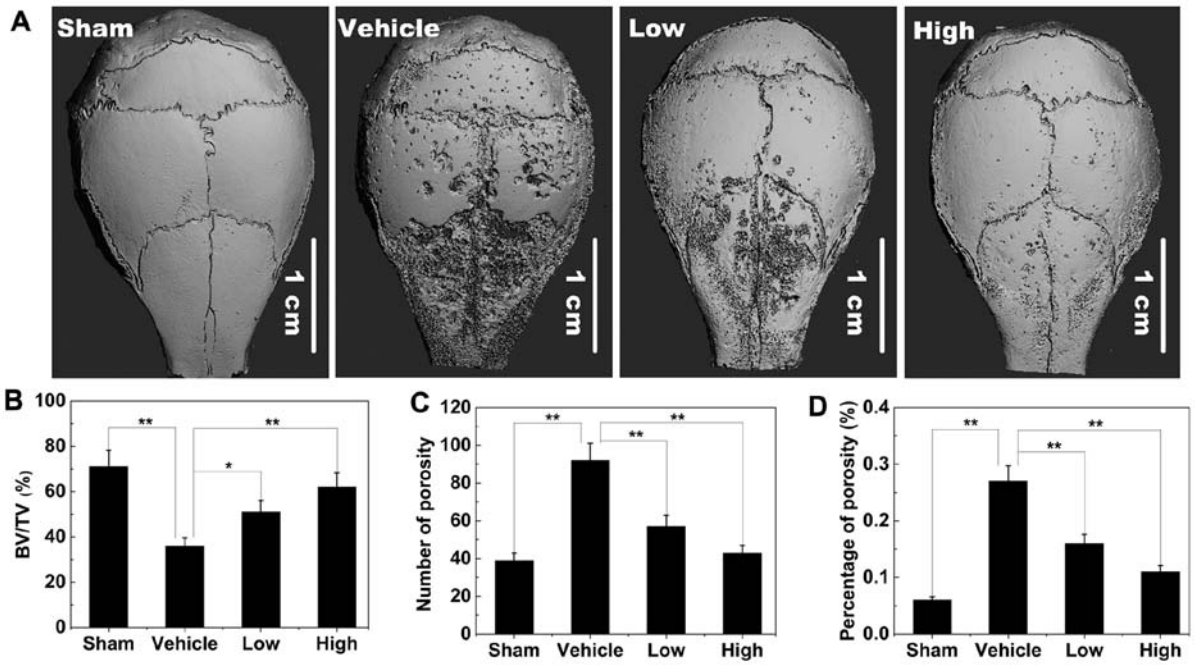

Figure 8. Astragaloside IV attenuates titanium particle-induced mouse calvarial osteolysis. (A) Representative micro-computed tomography three-dimensional reconstructed images from each group. (B) BV/TV, (C) number of porosities and (D) the percentage of total porosity in each sample. *P<0.05; **P<0.01. BV/TV, bone volume against tissue volume.

Ti particles, this osteolytic bone loss reduced (Fig. 8A). Quantitative analysis of bone parameters further demonstrated that the high or low concentrations of AS-IV significantly increased the BV/TV (Fig. 8B), and decreased the number of porosities and the percentage of total porosity in the ROI in the calvaria (Fig. 8C and D).

Discussion

Diseases associated with osteoclasts include osteoporosis, rheumatoid arthritis, multiple myeloma, periprosthetic osteolysis and metastatic cancers (2,44-46). During the last two decades, numerous advances have been made in the treatment of osteoclast-related diseases; however, treatment options are not optimal thus far.

The bisphosphonates were the first drugs approved specifically for the treatment and prevention of osteoclast-related diseases. However, they often cause gastrointestinal toxicity, including dyspepsia, abdominal pain, gastritis and esophagitis. Other serious adverse effects include osteonecrosis of the jaw, femur fractures and atrial fibrillation (47). Estrogens have also been used for the treatment of osteoporosis, but can have serious adverse effects, such as breast cancer, endometrial cancer and thromboembolism (48). The first effective bone anabolic agent teriparatide [parathyroid hormone (PTH) 1-34] has also been used clinically. However, high cost and the requirement for daily subcutaneous injections are major limitations to its use (49). Denosumab is a human monoclonal antibody that inhibits RANKL and, consequently, osteoclastogenesis. However, cellulitis was more frequent in patients taking denosumab compared with the placebo (50) and patients also had a high risk of fractures (51). Strontium ranelate is also used clinically; however, it has the common side effects of nausea, diarrhea, and mild and transient elevation in creatine kinase, and is contraindicated in patients with a high risk of thromboembolic events. In addition, a few cases of hypersensitivity have been reported (52). Due to the limitations of present therapies, attempts to develop improved treatment options are being pursued.

Previous studies indicated that AS-IV had positive effects on osteogenesis (32) and arthritis (33), and to the best of our knowledge, the present study demonstrated for the first time that it significantly inhibited osteoclast differentiation and formation, impaired F-actin ring formation, and significantly decreased the number and area of bone resorption pits *in vitro*. In the *in vivo* studies, three-dimensional reconstruction of micro-CT images from mouse calvarias showed that AS-IV treatment markedly suppressed Ti particle-induced osteolysis in a dose-dependent manner.

Activation of RANK by its ligand leads to the expression of osteoclast-specific genes during differentiation, and the activation of resorption by mature osteoclasts (11). RANK signaling is mediated by cytoplasmic factors that activate downstream pathways controlling these various functions. At least five distinct protein kinase-mediated signaling cascades are induced during osteoclastogenesis and activation; inhibitor of NF-κB kinase (IKK), c-Jun N-terminal kinase, p38, ERK and Src pathways (11). ERK is essential for osteoclast differentiation, survival and activation (16,17,53,54). The inhibition of ERK has been proven to possess a therapeutic potential for osteoclast-related diseases (39). Activated ERK stimulates transcription factors, such as NFATc1 (15), which is a master regulator of osteoclast differentiation (40,55,56). Overexpression of NFATc1 accelerates RANKL-induced osteoclast differentiation and can also increase osteoclast formation independently of RANKL. Additionally, NFATc1-deficient embryonic stem cells failed to differentiate into osteoclasts, even in the presence of RANKL (40). Using western blot analysis, AS-IV was revealed to inhibit RANKL-induced ERK signaling. NF-κB was unaffected and this result was confirmed using an NF-κB luciferase reporter assay. AS-IV also inhibited NFATc1 mRNA and protein expression. NFATc1 regulates the expression of a range of genes associated with osteoclast differentiation and function. In the present study, the expression of NFATc1-regulated genes (TRAP, CtsK and V-ATPase d2) was downregulated by AS-IV, suggesting that AS-IV not only affected the expression of NFATc1, but also affected the expression of its downstream genes.

In conclusion, the present study demonstrated that AS-IV had inhibitory effects on osteoclastogenesis and osteoclast function *in vitro* and *in vivo*. Additionally, these inhibitory effects appeared to operate via blockade of the ERK and NFATc1 pathways. Taken together, the data strongly suggested that AS-IV may be developed as a potential agent for the treatment of osteoclast-related diseases, including osteoporosis.

Acknowledgements

The present study was supported by the Department of Oncology, The First Affiliated Hospital of Zhengzhou University.

References

1. Kim HS, Suh KS, Sul D, Kim BJ, Lee SK and Jung WW: The inhibitory effect and the molecular mechanism of glabridin on RANKL-induced osteoclastogenesis in RAW264.7 cells. Int J Mol Med 29: 169-177, 2012.
2. Rodan GA and Martin TJ: Therapeutic approaches to bone diseases. Science 289: 1508-1514, 2000.
3. Kim TH, Kim HJ, Lee SH and Kim SY: Potent inhibitory effect of *Foeniculum vulgare* Miller extract on osteoclast differentiation and ovariectomy-induced bone loss. Int J Mol Med 29: 1053-1059, 2012.
4. Guo H, Zhang J, Hao S and Jin Q: Adenovirus-mediated small interfering RNA targeting tumor necrosis factor-α inhibits titanium particle-induced osteoclastogenesis and bone resorption. Int J Mol Med 32: 296-306, 2013.
5. Hou GQ, Guo C, Song GH, Fang N, Fan WJ, Chen XD, Yuan L and Wang ZQ: Lipopolysaccharide (LPS) promotes osteoclast differentiation and activation by enhancing the MAPK pathway and COX-2 expression in RAW264.7 cells. Int J Mol Med 32: 503-510, 2013.
6. Kanis JA and Kanis JA; WHO Study Group: Assessment of fracture risk and its application to screening for postmenopausal osteoporosis: Synopsis of a WHO report. Osteoporos Int 4: 368-381, 1994.
7. Udagawa N, Takahashi N, Akatsu T, Tanaka H, Sasaki T, Nishihara T, Koga T, Martin TJ and Suda T: Origin of osteoclasts: Mature monocytes and macrophages are capable of differentiating into osteoclasts under a suitable microenvironment prepared by bone marrow-derived stromal cells. Proc Natl Acad Sci USA 87: 7260-7264, 1990.
8. Purdue PE, Koulouvaris P, Potter HG, Nestor BJ and Sculco TP: The cellular and molecular biology of periprosthetic osteolysis. Clin Orthop Relat Res 454: 251-261, 2007.
9. Ren W, Wu B, Peng X, Hua J, Hao HN and Wooley PH: Implant wear induces inflammation, but not osteoclastic bone resorption, in RANK(-/-) mice. J Orthop Res 24: 1575-1586, 2006.
10. Raggatt LJ and Partridge NC: Cellular and molecular mechanisms of bone remodeling. J Biol Chem 285: 25103-25108, 2010.
11. Boyle WJ, Simonet WS and Lacey DL: Osteoclast differentiation and activation. Nature 423: 337-342, 2003.
12. Asagiri M and Takayanagi H: The molecular understanding of osteoclast differentiation. Bone 40: 251-264, 2007.
13. Strait K, Li Y, Dillehay DL and Weitzmann MN: Suppression of NF-kappaB activation blocks osteoclastic bone resorption during estrogen deficiency. Int J Mol Med 21: 521-525, 2008.

14. Zwerina J, Hayer S, Redlich K, Bobacz K, Kollias G, Smolen JS and Schett G: Activation of p38 MAPK is a key step in tumor necrosis factor-mediated inflammatory bone destruction. Arthritis Rheum 54: 463-472, 2006.
15. Meissner JD, Freund R, Krone D, Umeda PK, Chang KC, Gros G and Scheibe RJ: Extracellular signal-regulated kinase 1/2-mediated phosphorylation of p300 enhances myosin heavy chain I/beta gene expression via acetylation of nuclear factor of activated T cells c1. Nucleic Acids Res 39: 5907-5925, 2011.
16. Grigoriadis AE, Wang ZQ, Cecchini MG, Hofstetter W, Felix R, Fleisch HA and Wagner EF: c-Fos: A key regulator of osteoclast-macrophage lineage determination and bone remodeling. Science 266: 443-448, 1994.
17. Mansky KC, Sankar U, Han J and Ostrowski MC: Microphthalmia transcription factor is a target of the p38 MAPK pathway in response to receptor activator of NF-kappa B ligand signaling. J Biol Chem 277: 11077-11083, 2002.
18. Kim YW, Baek SH, Lee SH, Kim TH and Kim SY: Fucoidan, a sulfated polysaccharide, inhibits osteoclast differentiation and function by modulating RANKL signaling. Int J Mol Sci 15: 18840-18855, 2014.
19. Xuying W, Jiangbo Z, Yuping Z, Xili M, Yiwen Z, Tianbao Z and Weidong Z: Effect of astragaloside IV on the general and peripartum reproductive toxicity in Sprague-Dawley rats. Int J Toxicol 29: 505-516, 2010.
20. Ren S, Zhang H, Mu Y, Sun M and Liu P: Pharmacological effects of astragaloside IV: A literature review. J Tradit Chin Med 33: 413-416, 2013.
21. Jia Y, Zuo D, Li Z, Liu H, Dai Z, Cai J, Pang L and Wu Y: Astragaloside IV inhibits doxorubicin-induced cardiomyocyte apoptosis mediated by mitochondrial apoptotic pathway via activating the PI3K/Akt pathway. Chem Pharm Bull (Tokyo) 62: 45-53, 2014.
22. Tan S, Wang G, Guo Y, Gui D and Wang N: Preventive effects of a natural anti-inflammatory agent, astragaloside IV, on ischemic acute kidney injury in rats. Evid Based Complement Alternat Med 2013: 284025, 2013.
23. Hu JY, Han J, Chu ZG, Song HP, Zhang DX, Zhang Q and Huang YS: Astragaloside IV attenuates hypoxia-induced cardiomyocyte damage in rats by upregulating superoxide dismutase-1 levels. Clin Exp Pharmacol Physiol 36: 351-357, 2009.
24. Huang X, Tang L, Wang F and Song G: Astragaloside IV attenuates allergic inflammation by regulation Th1/Th2 cytokine and enhancement CD4(+)CD25(+)Foxp3 T cells in ovalbumin-induced asthma. Immunobiology 219: 565-571, 2014.
25. Qi H, Wei L, Han Y, Zhang Q, Lau AS and Rong J: Proteomic characterization of the cellular response to chemopreventive triterpenoid astragaloside IV in human hepatocellular carcinoma cell line HepG2. Int J Oncol 36: 725-735, 2010.
26. He CL, Yi PF, Fan QJ, Shen HQ, Jiang XL, Qin QQ, Song Z, Zhang C, Wu SC, Wei XB, *et al*: Xiang-Qi-Tang and its active components exhibit anti-inflammatory and anticoagulant properties by inhibiting MAPK and NF-κB signaling pathways in LPS-treated rat cardiac microvascular endothelial cells. Immunopharmacol Immunotoxicol 35: 215-224, 2013.
27. Wang Q, Shao X, Xu W, Qi C, Gu L, Ni Z and Mou S: Astragalosides IV inhibits high glucose-induced cell apoptosis through HGF activation in cultured human tubular epithelial cells. Ren Fail 36: 400-406, 2014.
28. Zheng R, Deng Y, Chen Y, Fan J, Zhang M, Zhong Y, Zhu R and Wang L: Astragaloside IV attenuates complement membranous attack complex induced podocyte injury through the MAPK pathway. Phytother Res 26: 892-898, 2012.
29. Gui D, Huang J, Guo Y, Chen J, Chen Y, Xiao W, Liu X and Wang N: Astragaloside IV ameliorates renal injury in streptozotocin-induced diabetic rats through inhibiting NF-κB-mediated inflammatory genes expression. Cytokine 61: 970-977, 2013.
30. Li M, Yu L, She T, Gan Y, Liu F, Hu Z, Chen Y, Li S and Xia H: Astragaloside IV attenuates Toll-like receptor 4 expression via NF-κB pathway under high glucose condition in mesenchymal stem cells. Eur J Pharmacol 696: 203-209, 2012.
31. Sun L, Li W, Li W, Xiong L, Li G and Ma R: Astragaloside IV prevents damage to human mesangial cells through the inhibition of the NADPH oxidase/ROS/Akt/NF-κB pathway under high glucose conditions. Int J Mol Med 34: 167-176, 2014.
32. Bian Q, Huang JH, Liang QQ, Shu B, Hou W, Xu H, Zhao YJ, Lu S, Shi Q and Wang YJ: The osteogenetic effect of astragaloside IV with centrifugating pressure on the OCT-1 cells. Pharmazie 66: 63-68, 2011.
33. Wang B and Chen MZ: Astragaloside IV possesses antiarthritic effect by preventing interleukin 1β-induced joint inflammation and cartilage damage. Arch Pharm Res 37: 793-802, 2014.
34. Xie J, Wang H, Song T, Wang Z, Li F, Ma J, Chen J, Nan Y, Yi H and Wang W: Tanshinone IIA and astragaloside IV promote the migration of mesenchymal stem cells by up-regulation of CXCR4. Protoplasma 250: 521-530, 2013.
35. Qin A, Cheng TS, Lin Z, Cao L, Chim SM, Pavlos NJ, Xu J, Zheng MH and Dai KR: Prevention of wear particle-induced osteolysis by a novel V-ATPase inhibitor saliphenylhalamide through inhibition of osteoclast bone resorption. PLoS One 7: e34132, 2012.
36. Wedemeyer C, Xu J, Neuerburg C, Landgraeber S, Malyar NM, von Knoch F, Gosheger G, von Knoch M, Löer F and Saxler G: Particle-induced osteolysis in three-dimensional micro-computed tomography. Calcif Tissue Int 81: 394-402, 2007.
37. Qin A, Cheng TS, Pavlos NJ, Lin Z, Dai KR and Zheng MH: V-ATPases in osteoclasts: Structure, function and potential inhibitors of bone resorption. Int J Biochem Cell Biol 44: 1422-1435, 2012.
38. Monje P, Hernández-Losa J, Lyons RJ, Castellone MD and Gutkind JS: Regulation of the transcriptional activity of c-Fos by ERK. A novel role for the prolyl isomerase PIN1. J Biol Chem 280: 35081-35084, 2005.
39. Seo SW, Lee D, Minematsu H, Kim AD, Shin M, Cho SK, Kim DW, Yang J and Lee FY: Targeting extracellular signal-regulated kinase (ERK) signaling has therapeutic implications for inflammatory osteolysis. Bone 46: 695-702, 2010.
40. Takayanagi H, Kim S, Koga T, Nishina H, Isshiki M, Yoshida H, Saiura A, Isobe M, Yokochi T and Inoue J: Induction and activation of the transcription factor NFATc1 (NFAT2) integrate RANKL signaling in terminal differentiation of osteoclasts. Dev Cell 3: 889-901, 2002.
41. Franzoso G, Carlson L, Xing L, Poljak L, Shores EW, Brown KD, Leonardi A, Tran T, Boyce BF and Siebenlist U: Requirement for NF-kappaB in osteoclast and B-cell development. Genes Dev 11: 3482-3496, 1997.
42. Iotsova V, Caamaño J, Loy J, Yang Y, Lewin A and Bravo R: Osteopetrosis in mice lacking NF-kappaB1 and NF-kappaB2. Nat Med 3: 1285-1289, 1997.
43. Lee SH, Kim JK and Jang HD: Genistein inhibits osteoclastic differentiation of RAW 264.7 cells via regulation of ROS production and scavenging. Int J Mol Sci 15: 10605-10621, 2014.
44. Inacio MC, Ake CF, Paxton EW, Khatod M, Wang C, Gross TP, Kaczmarek RG, Marinac-Dabic D and Sedrakyan A: Sex and risk of hip implant failure: Assessing total hip arthroplasty outcomes in the United States. JAMA Intern Med 173: 435-441, 2013.
45. Rizzoli R: A new treatment for post-menopausal osteoporosis: Strontium ranelate. J Endocrinol Invest 28 (Suppl): 50-57, 2005.
46. Weitzmann MN and Pacifici R: Estrogen regulation of immune cell bone interactions. Ann NY Acad Sci 1068: 256-274, 2006.
47. Marx RE: The deception and fallacies of sponsored randomized prospective double-blinded clinical trials: The bisphosphonate research example. Int J Oral Maxillofac Implants 29: e37-e44, 2014.
48. Maeda SS and Lazaretti-Castro M: An overview on the treatment of postmenopausal osteoporosis. Arq Bras Endocrinol Metabol 58: 162-171, 2014.
49. Nakamura T, Sugimoto T, Nakano T, Kishimoto H, Ito M, Fukunaga M, Hagino H, Sone T, Yoshikawa H, Nishizawa Y, *et al*: Randomized Teriparatide [human parathyroid hormone (PTH) 1-34] Once-Weekly Efficacy Research (TOWER) trial for examining the reduction in new vertebral fractures in subjects with primary osteoporosis and high fracture risk. J Clin Endocrinol Metab 97: 3097-3106, 2012.
50. Cummings SR, San Martin J, McClung MR, Siris ES, Eastell R, Reid IR, Delmas P, Zoog HB, Austin M, Wang A, *et al*; FREEDOM Trial: Denosumab for prevention of fractures in postmenopausal women with osteoporosis. N Engl J Med 361: 756-765, 2009.

51. Hiligsmann M, Boonen A, Dirksen CD, Ben Sedrine W and Reginster JY: Cost-effectiveness of denosumab in the treatment of postmenopausal osteoporotic women. Expert Rev Pharmacoecon Outcomes Res 13: 19-28, 2013.
52. Meunier PJ, Roux C, Ortolani S, Diaz-Curiel M, Compston J, Marquis P, Cormier C, Isaia G, Badurski J, Wark JD, *et al*: Effects of long-term strontium ranelate treatment on vertebral fracture risk in postmenopausal women with osteoporosis. Osteoporos Int 20: 1663-1673, 2009.
53. Gingery A, Bradley E, Shaw A and Oursler MJ: Phosphatidylinositol 3-kinase coordinately activates the MEK/ERK and AKT/NFkappaB pathways to maintain osteoclast survival. J Cell Biochem 89: 165-179, 2003.
54. Liu X, Qu X, Wu C, Zhai Z, Tian B, Li H, Ouyang Z, Xu X, Wang W, Fan Q, *et al*: The effect of enoxacin on osteoclastogenesis and reduction of titanium particle-induced osteolysis via suppression of JNK signaling pathway. Biomaterials 35: 5721-5730, 2014.
55. Zhai Z, Qu X, Li H, Yang K, Wan P, Tan L, Ouyang Z, Liu X, Tian B, Xiao F, *et al*: The effect of metallic magnesium degradation products on osteoclast-induced osteolysis and attenuation of NF-κB and NFATc1 signaling. Biomaterials 35: 6299-6310, 2014.
56. Liu F, Zhu Z, Mao Y, Liu M, Tang T and Qiu S: Inhibition of titanium particle-induced osteoclastogenesis through inactivation of NFATc1 by VIVIT peptide. Biomaterials 30: 1756-1762, 2009.